



**HAL**  
open science

# Single Cell Multiplex Reverse Transcription Polymerase Chain Reaction After Patch-clamp

Gabrielle Devienne, Benjamin Le Gac, Juliette Piquet, Bruno Cauli

► **To cite this version:**

Gabrielle Devienne, Benjamin Le Gac, Juliette Piquet, Bruno Cauli. Single Cell Multiplex Reverse Transcription Polymerase Chain Reaction After Patch-clamp. *Journal of visualized experiments: JoVE*, 2018, 136, pp.57627. 10.3791/57627 . hal-01961034

**HAL Id: hal-01961034**

**<https://hal.sorbonne-universite.fr/hal-01961034>**

Submitted on 19 Dec 2018

**HAL** is a multi-disciplinary open access archive for the deposit and dissemination of scientific research documents, whether they are published or not. The documents may come from teaching and research institutions in France or abroad, or from public or private research centers.

L'archive ouverte pluridisciplinaire **HAL**, est destinée au dépôt et à la diffusion de documents scientifiques de niveau recherche, publiés ou non, émanant des établissements d'enseignement et de recherche français ou étrangers, des laboratoires publics ou privés.

## Video Article

# Single Cell Multiplex Reverse Transcription Polymerase Chain Reaction After Patch-clamp

Gabrielle Devienne<sup>\*1</sup>, Benjamin Le Gac<sup>\*1</sup>, Juliette Piquet<sup>\*1</sup>, Bruno Cauli<sup>1</sup>

<sup>1</sup>UPMC Univ Paris 06, INSERM, CNRS, Neuroscience Paris Seine - Institut de Biologie Paris Seine (NPS - IBPS), Sorbonne Universités

\*These authors contributed equally

Correspondence to: Bruno Cauli at [bruno.cauli@upmc.fr](mailto:bruno.cauli@upmc.fr)

Keywords: Gene expression profile, neurons, astrocytes, brain slices, whole-cell configuration, nested polymerase chain reaction (PCR)

## Abstract

The cerebral cortex is composed of numerous cell types exhibiting various morphological, physiological, and molecular features. This diversity hampers easy identification and characterization of these cell types, prerequisites to study their specific functions. This article describes the multiplex single cell reverse transcription polymerase chain reaction (RT-PCR) protocol, which allows, after patch-clamp recording in slices, to detect simultaneously the expression of tens of genes in a single cell. This simple method can be implemented with morphological characterization and is widely applicable to determine the phenotypic traits of various cell types and their particular cellular environment, such as in the vicinity of blood vessels. The principle of this protocol is to record a cell with the patch-clamp technique, to harvest and reverse transcribe its cytoplasmic content, and to detect qualitatively the expression of a predefined set of genes by multiplex PCR. It requires a careful design of PCR primers and intracellular patch-clamp solution compatible with RT-PCR. To ensure a selective and reliable transcript detection, this technique also requires appropriate controls from cytoplasm harvesting to amplification steps. Although precautions discussed here must be strictly followed, virtually any electrophysiological laboratory can use the multiplex single cell RT-PCR technique.

## Video Link

The video component of this article can be found at <https://www.jove.com/video/57627/>

## Introduction

The cerebral cortex comprises numerous cell types involved in various physiological processes. Their identification and characterization, a prerequisite to the understanding of their specific functions, can be very challenging given the large morphological, physiological, and molecular diversity that characterizes cortical cell types<sup>1,2,3,4</sup>.

Single-cell multiplex RT-PCR is based on the combination of patch-clamp and RT-PCR techniques. It can probe simultaneously the expression of more than 30 predefined genes in electrophysiologically identified cells<sup>5</sup>. The inclusion of a neuronal tracer in the recording pipette further allows the morphological characterization of the recorded cells after histochemical revelation<sup>6,7,8,9,10</sup>. It is a very useful technique for the classification of neuronal types based on multivariate analysis of their phenotypic traits<sup>5,9,10,11,12,13,14</sup>. Single cell multiplex RT-PCR is also suited to the characterization of non-neuronal cells such as astrocytes<sup>15,16,17</sup>, and can be virtually applied to every brain structure<sup>18,19,20,21,22,23</sup> and cell type, assuming they can be recorded in whole-cell configuration.

This technique is very convenient for the identification of cellular sources and/or targets of transmission systems<sup>7,8,15,16,20,21,24,25,26,27,28</sup>, especially when specific antibodies are lacking. It relies on patch-clamp recordings from visually identified cells<sup>29</sup>, and thus also allows the targeting of cells in a specific cellular environment<sup>8,15,16</sup>. Furthermore since the cytoarchitecture of brain tissue is preserved in brain slices, this approach also enables study of the anatomical relationships of the characterized cells with neuronal and non-neuronal elements<sup>7,8,18</sup>.

Since this technique is limited by the amount of harvested cytoplasm and by the efficiency of the RT, the detection of mRNA expressed at low copy number can be difficult. Although other approaches based on RNaseq technology allow to analyze the whole transcriptome of single cells<sup>3,4,30,31</sup>, they need high-throughput expensive sequencers not necessarily available to every laboratory. Since the single cell multiplex RT-PCR technique uses end-point PCR, it only requires widely available thermocyclers. It can be easily developed in laboratories equipped with electrophysiological set-ups and does not require expensive equipment. It can provide, within one day, a qualitative analysis of the expression of a predefined set of genes. Thus, this approach offers an easy access to the molecular characterization of single cells in a rapid manner.

## Protocol

All experimental procedures using animals were performed in strict accordance with French regulations (Code Rural R214/87 to R214/130) and conformed to the ethical guidelines of both the European Economic Community (86/609/EEC) and the French National Charter on the ethics of

animal experimentation. All protocols were approved by the Charles Darwin ethics committee and submitted to the French Ministry of Education and Research (Approval 2015 061011367540). The IBPS animal facility is accredited by the French authorities (A75-05-24).

## 1. Preliminary Considerations

Note: To avoid contaminations, conform to the following recommendations before undertaking single cell RT-PCR after patch-clamp.

1. Do not use plasmids containing genes of interest in the laboratory as they are a potential source of contamination.
2. Reserve a lab bench away from the gel electrophoresis room to prepare PCRs.
3. Dedicate a set of pipettes and aerosol resistant filter tips to manipulate DNA and RNA at concentrations lower than 1 ng/μL. Never use these to analyze PCR products.
4. Always use RNase- and DNase-free products and wear gloves.
5. Use dedicated chemicals for preparing internal patch-clamp solutions. Never use a spatula but rather weighing paper to weigh powders.
6. Use a dedicated pH electrode and pH standard solutions, as they can be a source of contamination (e.g., RNase).
7. Store borosilicate glass capillaries; 20 μL long, fine and flexible tips; a 20 μL micropipette; a home-made expeller (patch-clamp pipette holder attached to a 10 mL syringe); 500 μL PCR tubes; 10 μL aerosol resistant filter tips; and thin permanent markers in a dedicated box (**Figure 1**).

## 2. Primer Design

Note: Multiplex RT-PCR relies on two amplification steps. During the first PCR, all the genes of interest are co-amplified by mixing together all PCR primers. To detect reliably transcripts from single cells, it is essential to design efficient and selective PCR primers. The use of nested (internal) primers for the second rounds of PCR improves both the specificity and the efficiency of the amplification.

1. Retrieve the curated mRNA sequences of the genes of interest in NCBI Reference Sequence Database<sup>32</sup> as well as those of their related family (<https://www.ncbi.nlm.nih.gov/refseq/>).
  1. Enter the name of the gene(s) and the species of interest as a query and click on the retrieved relevant sequence.
  2. To restrict the analysis to the coding sequence of the gene(s), click on **Send to** (upper right corner), and select **Coding sequences** and **FASTA Nucleotide** as format. Then click on **Create File** and save the FASTA sequence using a ".nt" file extension.
2. Use MACAW software<sup>33</sup> (Multiple Alignment Construction & Analysis Workbench) or any other multiple alignment software to determine the regions of homology.
  1. Click on **File | New Project...** and select **DNA** as the sequence type. To import the gene sequences, select **Sequence | Import Sequence...** and load a ".nt" file. Repeat the procedure for all related sequences.
  2. Click and drag all sequences in the **Schematic** window to select the entire sequences.
  3. Search the regions of homology by selecting **Alignment | Search for Blocks...** (CTRL+S). Select **Segment pair overlap** in **Search Method**. Adjust the **Pairwise score cutoff** to a relatively high value (e.g., 1,000) and the **Min. seqs. per block** to the total number of sequences to align and click on **Begin**.
  4. In the appearing **Search Result** window, select the result(s) with the highest MP-score and click on **Link**. If no result is found, decrease the **Pairwise score cutoff** and/or the **Min. seqs. per block**.
  5. To facilitate the visualization of homologous regions, select **Alignment | Shading | Mean score**.
  6. Select unlinked parts of the sequences and repeat the steps 2.2.3–2.2.4 to potentially determine other regions of homology with a lower MP-score.
  7. To obtain the most specific primers, select the regions with the least sequence homology.
3. Fetch the sequences of all splice variants and repeat steps 2.2.1–2.2.6. Select their common regions for an overall detection. Consider alternative cassettes for dedicated splice variants analyses<sup>20,34,35,36</sup>
4. Align the mRNA sequences on the animal model genome using BLAST<sup>37</sup> genomes (Basic Local Alignment Search Tool) to determine the intron-exon structure of the genes (<https://blast.ncbi.nlm.nih.gov/Blast.cgi>).
  1. Select the BLAST mouse genome by clicking on **Mouse** and upload the retrieved FASTA sequence in the **Enter Query Sequence** section. In the **Program Selection**, select **Optimize for Highly similar sequences (megablast)**, then click on the **BLAST** button.
  2. In the **Descriptions** section, select the alignment with the highest Identity (up to 100%). Make sure that it corresponds to the gene of interest as indicated in **features** of the **Alignments** section.
  3. Sort the alignment by **Query start position** in the same section to obtain the exons succession of the coding sequence. Note the start and end positions of all hits which roughly correspond to the position of the introns on the query sequence (**Figure 2A**).
5. Select two different exons for the sense and antisense primers to differentiate easily cDNA from genomic DNA (gDNA) amplification based on a size criterion (**Figure 2**).

Note: The amplification of gDNA can occur at a low frequency when the nucleus is harvested with the cytoplasm. Thus, it is essential to design intron overspanning primer pairs (**Figure 2A**). In case of intron-less genes, the collection of the nucleus is problematic as it can lead to potentially confounding results. To address this issue, include a set of primers aimed at amplifying an intronic sequence to probe for the presence of gDNA<sup>25</sup>. If the genomic control is positive, the results for all intron-less genes must be discarded.
6. To achieve an efficient amplification, select primers generating amplicons with a length ideally comprised between 200 and 400 base pairs (**Figure 2**).
7. To amplify simultaneously various cDNAs during the multiplex PCR step, design primers with a length between 18 and 24 nucleotides and a melting temperature (T<sub>m</sub>) between 55 and 60 °C.
8. To minimize the formation of secondary structures, which reduce the amplification yield, select sense and anti-sense primers with minimal hairpin and duplex lengths (**Figure 2B**).
9. Design internal primers using the same criteria (steps 2.5–2.8).

10. Verify the specificity of the PCR primers by aligning the primers on the Reference RNA Sequence Database of the organism of interest using a nucleotide BLAST.
  1. In BLAST (<https://blast.ncbi.nlm.nih.gov/Blast.cgi>), click on **nucleotide BLAST**. Paste the sequence of a primer in the **Enter Query Sequence**.
  2. In the **Choose Search Set** section, click on **Others (nr etc.)**, select **Reference RNA sequences (refseq\_rna)** in the **Database** option and specify the organism (e.g., *Mus musculus* (taxid:10090)) to restrict the analysis to the desired species.
  3. In **Program Selection** select **Optimize for Somewhat similar sequences (blastn)**. In the **Algorithm parameters** section reduce the **word size** down to 7 to increase the chance to obtain hits.
11. To design selective primers, keep only those whose sequence has at least 3 mismatches with undesired cDNAs when possible.
12. Order desalted primers at a relatively high concentration (e.g., 200  $\mu\text{M}$ ) to ensure that all external primers can be mixed together at a final concentration of 1  $\mu\text{M}$ .

### 3. Preparation of RT Reagents

1. 5x RT-mix: Prepare in RNase-free water 400  $\mu\text{L}$  of working RT mix solution (5x) containing random primers at 25  $\mu\text{M}$  and dNTPs at 2.5 mM each. Store this working mix as 20  $\mu\text{L}$  aliquots in 500  $\mu\text{L}$  tubes.
2. 20x Dithiothreitol (DTT): Prepare 1 mL of 0.2 M DTT in RNase-free water and store it as 50  $\mu\text{L}$  aliquots.
3. Store 2,500 U of RNase inhibitor (40 U/ $\mu\text{L}$ ) and 10,000 U of reverse transcriptase (RTase, 200 U/ $\mu\text{L}$ ) as 5  $\mu\text{L}$  aliquots.
4. To ensure an optimal quality of the RT reagents, store the aliquots at  $-80\text{ }^{\circ}\text{C}$ . Use them for up to 10 cells and only for one day.

### 4. PCR Validation

1. Prepare cDNAs by doing a reverse transcription on a relatively large amount of total RNA (typically 1  $\mu\text{g}$ ) extracted<sup>38</sup> from the structure of interest.
  1. Do not use the pipettes dedicated to single cell RT-PCR for these preliminary steps but use the RNase-free pipettes. Dilute total RNA down to 1  $\mu\text{g}/\mu\text{L}$ .
  2. In a 500  $\mu\text{L}$  PCR tube, add 1  $\mu\text{L}$  of diluted total RNA and 8  $\mu\text{L}$  of RNase-free water. Denature at  $95\text{ }^{\circ}\text{C}$  for 1 min and cool down the tube on ice.
  3. Add 4  $\mu\text{L}$  of RT 5x buffer supplied by the manufacturer, 4  $\mu\text{L}$  of RT mix solution, 1  $\mu\text{L}$  of RTase, 1  $\mu\text{L}$  of RNase inhibitor, and 1  $\mu\text{L}$  of 200 mM DTT (see Section 3).
  4. Flick the tube, spin it, and incubate overnight at  $37\text{ }^{\circ}\text{C}$ .
  5. Store the cDNAs at  $-80\text{ }^{\circ}\text{C}$  for up to several years. Prepare an aliquot of cDNAs diluted to 1 ng/ $\mu\text{L}$  of total RNAs equivalents.
2. Mix and dilute each primer pair at 1  $\mu\text{M}$  with the pipettes dedicated to single cell RT-PCR. Use 20  $\mu\text{L}$  of each primer mix for 100  $\mu\text{L}$  PCRs.
3. On ice, prepare for each primer pair a premix containing: water (*q.s.*, 80  $\mu\text{L}$ ), 10  $\mu\text{L}$  of 10X buffer, 1  $\mu\text{L}$  of 100x dNTPs (50  $\mu\text{M}$  each), 500–1,000 pg of cDNA diluted at 1 ng/ $\mu\text{L}$ , and 0.5  $\mu\text{L}$  (2.5 U, 5 U/ $\mu\text{L}$ ) of Taq polymerase.
4. Use PCR tubes that tightly fit the wells of the PCR machine for an optimal temperature control. Add 2 drops (~100  $\mu\text{L}$ ) of mineral oil to the premix without touching the wall or the cap of the PCR tube.
5. To minimize the formation of primer-dimers, perform a hot start by placing the PCR tubes in the thermocycler pre-heated at  $95\text{ }^{\circ}\text{C}$ . After 30 s, quickly expel 20  $\mu\text{L}$  of the primer mix on top of the oil.
6. After 3 min at  $95\text{ }^{\circ}\text{C}$ , run 40 cycles ( $95\text{ }^{\circ}\text{C}$ , 30 s;  $60\text{ }^{\circ}\text{C}$ , 30 s;  $72\text{ }^{\circ}\text{C}$ , 35 s) followed by a final elongation step at  $72\text{ }^{\circ}\text{C}$  for 5 min.
7. Analyze 10  $\mu\text{L}$  of each PCR products by agarose gel electrophoresis (2%, weight/volume)<sup>39</sup>. If some PCR products do not have the expected size, re-design other primers (see Section 2).
 

Caution: Ethidium bromide is an intercalating chemical that can induce DNA mutations. Consult the local safety office before using it. Always wear gloves when manipulating it. Use a commercially available solution of ethidium bromide (10 mg/mL) solution instead of powder to minimize the risk of inhalation. Similarly, UV light can be harmful, so make sure to wear UV protection safety glasses or a mask. Withdraw soiled gels, tips, gloves, and buffer in containers dedicated to ethidium waste.
8. Once all primer pairs have been individually validated, test the multiplex protocol (**Figure 3**).
  1. Mix and dilute all external primers together at 1  $\mu\text{M}$ . Store the multiplex primers mix at  $-20\text{ }^{\circ}\text{C}$  for up to several weeks.
  2. On ice, prepare a premix containing: water (*q.s.*, 80  $\mu\text{L}$ ), 10  $\mu\text{L}$  of 10X buffer, 1  $\mu\text{L}$  of 100x dNTPs (50  $\mu\text{M}$  of each), 500–1,000 pg of cDNAs diluted at 1 ng/ $\mu\text{L}$ , and 0.5  $\mu\text{L}$  (2.5 U, 5 U/ $\mu\text{L}$ ) of Taq polymerase.
  3. Flick the PCR tube, spin it, and add two drops (~100  $\mu\text{L}$ ) of mineral oil.
  4. Perform a hot start as described in step 4.5 with 20  $\mu\text{L}$  of multiplex primer mix. After 3 min at  $95\text{ }^{\circ}\text{C}$ , run 20 PCR cycles identical to those of step 4.6.
  5. Prepare a number of PCR tubes identical to the number of genes to analyze. Prepare a premix as in step 4.8.2, but using 1  $\mu\text{L}$  of the first PCR product per gene as template. Adjust all the volumes according to the number of genes to analyze and consider using 10% of extra volume to compensate for pipetting errors.
  6. Shake gently, spin the tube, dispatch 80  $\mu\text{L}$  of premix in each PCR tube, and add two drops (~100  $\mu\text{L}$ ) of mineral oil per tube without touching the wall or the cap of the tubes.
  7. Perform a hot start (see step 4.5) by expelling 20  $\mu\text{L}$  of internal primer mix prepared in step 4.2. Run 35 PCR cycles identical to step 4.6.
  8. Analyze the second PCR products by agarose gel electrophoresis. Make sure that every second PCR generates an amplicon of the expected size. In case of inefficient or nonspecific amplifications, re-design new primers (steps 2.5–2.12) and validate them (steps 4.2–4.8).

## 5. Preparation and Validation of Intracellular Patch-clamp Solution

Note: The following protocol describes the preparation and validation of a  $K^+$ /gluconate based internal solution, but virtually any type of patch-clamp solution can be used as long as it does not hamper the efficiency of the RT-PCR. Wearing gloves is mandatory to obtain an RNase-free internal solution.

1. For 60 mL of internal patch-clamp recording solution, prepare extemporaneously 10 mL of 0.1 M KOH.
2. Dissolve 11.4 mg of EGTA (0.5 mM final) in 0.9 mL of 0.1 M KOH.
3. Add 40 mL RNase-free water and dissolve 2.02 g of K-gluconate (144 mM final), 143 mg of HEPES (10 mM final), and 180  $\mu$ L of 1 M  $MgCl_2$  (3 mM final).
4. Adjust the pH to 7.2 by adding ~6 mL of 0.1 M KOH.
5. Adjust the osmolarity to 295 mOsm with ~13 mL of RNase-free water.
6. Since the internal solution is also used as a buffer for the reverse transcription, carefully control  $Mg^{2+}$  concentration. Compensate for a lower  $Mg^{2+}$  concentration in the internal solution by adding  $MgCl_2$  afterwards to reach a final concentration of 2 mM in the RT reaction.
7. To label the harvested cell after patch-clamp recording, add 2–5 mg/mL of RNase-free biocytin to the internal solution described above (steps 5.1–5.5).
8. Filter (0.22  $\mu$ m pore size) the internal solution and store it at -80 °C as 100–250  $\mu$ L aliquots.
9. To validate the use of the internal solution for single-cell RT-PCR, add 0.5  $\mu$ L of total RNAs diluted at 1 ng/ $\mu$ L to 6  $\mu$ L of patch-clamp solution and leave it on the bench for about 30 min.
10. With a 2  $\mu$ L micropipette, add 2  $\mu$ L of 5x RT-mix, 0.5  $\mu$ L of 20x DDT, 0.5  $\mu$ L RNase inhibitor, and 0.5  $\mu$ L RTase, and incubate overnight at 37 °C.
11. Spin the tube. On ice add water (*q.s.*, 80  $\mu$ L), 10  $\mu$ L of 10X buffer, and 0.5  $\mu$ L (2.5 U, 5 U/ $\mu$ L) of Taq polymerase.
12. Perform 40 cycles of PCR using a set of validated primers (steps 4.4–4.6).
13. Analyze the PCR products by agarose gel electrophoresis (see step 4.7) and verify that they have the expected size.  
Note: Omitting the 0.5  $\mu$ L of total RNA and replacing it with 0.5  $\mu$ L RNase-free water will ensure that the internal solution is free of RNA and/or DNA contaminations.

## 6. Acute Slice Preparation

Note: This protocol describes the slicing procedure for juvenile (*i.e.*, less than 28 postnatal days) male and female mice. Other cutting solutions, such as sucrose-based artificial cerebrospinal fluid (aCSF) are also usable<sup>40</sup>.

1. Prepare 2 L of aCSF containing (in mM) 125 NaCl, 2.5 KCl, 2  $CaCl_2$ , 1  $MgCl_2$ , 1.25  $NaH_2PO_4$ , 26  $NaHCO_3$ , 10 Glucose, and 15 Sucrose. To reduce glutamatergic activity during slice preparation, prepare a cutting solution by adding 1 mM of kynurenic acid.
2. Before slicing, prepare a dissection kit containing surgical scissors, fine iris scissors, two spatulas, forceps, a disc of paper filter, and cyanoacrylate glue.
3. Use ice-cold cutting solution saturated with  $O_2/CO_2$  (95%/5%) and cool down the cutting chamber at -20 °C.
4. Anesthetize the mouse with a small paper towel soaked with isoflurane. After ~2 min, make sure that the mouse is under deep anesthesia by verifying the absence of response to paw pinch.
5. Quickly decapitate the mouse. Remove the scalp and open the skull. Extract the brain carefully and place it into a small beaker filled with ice cold (~4 °C) cutting solution oxygenated with  $O_2/CO_2$ .
6. Remove the cutting chamber from -20 °C conditions and remove moisture with a paper towel.
7. Carefully dissect the brain to isolate the region of interest, glue it on the cutting chamber, and add ice-cold cutting solution oxygenated with  $O_2/CO_2$ .
8. Cut 300  $\mu$ m thick slices using a vibratome. Transfer them at room temperature in a resting chamber filled with oxygenated cutting solution and allow them to recover for at least 0.5 h.

## 7. Single Cell RT-PCR after Patch-clamp Recording

1. Clean the perfusion system regularly with ~100 mL of 30%  $H_2O_2$  solution and rinse extensively with ~500 mL of distilled water to avoid bacteria growth, as it is an overlooked source of RNase contamination.
2. Chlorinate the filament with a patch pipette filled with concentrated bleach every harvesting day. Do not use a micropipette to fill the patch pipette but rather a 20  $\mu$ L long, fine, flexible tip attached to a 1 mL syringe. Then, rinse it extensively with RNase free water and dry it with a gas duster.
3. Prepare a small box of ice containing 5x RT-mix and 20x DTT aliquots. Store the RTase and RNase inhibitor aliquots at -20 °C in a benchtop cooler.
4. Transfer a slice into the recording chamber perfused at 1–2 mL/min with oxygenated aCSF.
5. Pull patch pipettes (1–2  $\mu$ m open tip diameter, 3–5 M $\Omega$ ) from borosilicate glass while wearing gloves and fill one of them with 8  $\mu$ L of internal solution. Keep in mind that the knobs of the pipette puller are a source of RNase contamination.
6. Place the pipette in the pipette holder while wearing new gloves and not touching the filament with fingers.
7. Approach the patch pipette with a positive pressure and perform whole-cell recording to characterize the targeted cell (**Figure 4**).
8. 7.8. In order to preserve the mRNAs, limit the time in whole-cell configuration to 20 min<sup>41</sup>.
9. At the end of the recording, prepare a 500  $\mu$ L PCR tube filled with 2  $\mu$ L of 5x RT Mix and 0.5  $\mu$ L of 20x DTT, spin it, and store it on ice.
10. Harvest the cell cytoplasm by applying a gentle negative pressure (**Figure 4**). Visually control that the cell's content comes inside the pipette while maintaining a tight seal.
  1. Avoid as much as possible collecting the nucleus if some intron-less genes are considered. In such a case always include a set of primers aimed at amplifying gDNA to probe for genomic contamination.

2. If the nucleus is coming close to the tip of the pipette, release the negative pressure and move the pipette away from the nucleus. Ensure that the tight seal is preserved and restart to collect the cytoplasm at the new pipette location.
11. Stop the harvesting when no more material is coming and/or before losing the tight seal.
12. Withdraw the pipette gently to form an outside-out patch to limit contamination by the extracellular debris (**Figure 4**) and to favor the closure of the cell membrane for subsequent histochemical analysis.
13. Keep in mind that knobs, micromanipulators, computer keyboard, or computer mouse are potential sources of RNase contamination. If they have been touched during the recording, change gloves.
14. Attach the pipette to the expeller and expel its content into the PCR tube by applying a positive pressure (**Figure 1**).
15. Break the tip of the pipette into the PCR tube to help the collection of its content.
16. Briefly centrifuge the tube, add 0.5  $\mu$ L of RNase inhibitor and 0.5  $\mu$ L of RTase, mix gently, centrifuge again, and incubate overnight at 37 °C.
17. Spin the tube and store it at -80 °C for up to several months until PCR analysis.
18. Perform the first amplification step directly in the tube containing the ~10  $\mu$ L of RT products by adding water (*q.s.*, 80  $\mu$ L), 10  $\mu$ L of 10x buffer, and 0.5  $\mu$ L (2.5 U) of Taq polymerase. Then, follow the instructions described in steps 4.8.2–4.8.8.

## 8. Histochemical Staining of the Recorded Cell (Optional)

1. Following the electrophysiological recordings, maintain the slice for 20 min in oxygenated aCSF to allow the diffusion of biocytin in the axonal and dendritic tree.
2. Place the slice in a well of a 24-well plate and fix it overnight at 4 °C with 1 mL of 4% paraformaldehyde in 0.1 M Phosphate Buffer.
3. Wash the slices 4 times, 5 min each, with 1 mL Phosphate Buffered Saline (PBS).
4. In the same well, permeabilize and saturate the slice during 1 h at room temperature with 1 mL of PBS supplemented with 0.25% Triton X-100 and 0.2% gelatin from cold water fish skin (PBS-GT).
5. Incubate overnight with a fluorescently labeled avidin diluted at 1/400 in 250–500  $\mu$ L of PBS-GT.
6. Wash 5 times, 5 min each, with 1 mL of PBS and mount the slices.

## Representative Results

A representative validation of multiplex RT-PCR is shown in **Figure 3**. The protocol was designed to probe simultaneously the expression of 12 different genes. The vesicular glutamate transporter vGluT1 was taken as a positive control for glutamatergic neurons<sup>42</sup>. The GABA synthesizing enzymes (GAD65 and GAD 67), Neuropeptide Y (NPY), and Somatostatin (SOM) were used as markers of GABAergic interneurons<sup>3,5,11</sup>. The cyclooxygenase-2 enzyme (COX-2) was used as a marker of the pyramidal cell sub-population<sup>3,16</sup>.

The ATP1 $\alpha$ 1-3 subunits of the Na<sup>+</sup>/K<sup>+</sup> ATPase and the Kir6.2 and SUR1 subunits of the ATP-sensitive K<sup>+</sup> channels were chosen to evaluate the relationship between neuronal activity and metabolic states<sup>43</sup>. Since Kir6.2 is an intron-less gene, the SOM intron was included as a genomic control. The protocol has been tested on 1 ng of reverse transcribed total RNA extracted from mouse whole brain, which corresponds approximately to the transcripts of 20 cells<sup>44</sup>. The multiplex PCR produced 12 amplicons of the expected size (**Figure 3** and **Table 1**) demonstrating the sensitivity and efficiency of the protocol. The negative control performed without RNA produced no amplicon (data not shown).

A layer V pyramidal neuron was visually identified by its large soma and a prominent apical dendrite (**Figure 5A**, inset). Whole cell recording revealed typical electrophysiological properties of layer V regular spiking neurons<sup>5,45,46</sup> with, notably, a low input resistance, long-lasting action potentials, and pronounced spike frequency adaptation (**Figure 5A**). The molecular analysis of this neuron revealed the expression of vGluT1 (**Figure 5B**), confirming its glutamatergic phenotype<sup>42,46</sup>. This neuron also expressed SOM, ATP1 $\alpha$ 1, and 3 subunits of the Na<sup>+</sup>/K<sup>+</sup> ATPase. Biocytin labeling of the recorded neurons confirmed a pyramidal morphology (**Figure 5D**).

As expected from glutamatergic neurons, the molecular analysis of 26 layer V pyramidal cells revealed expression of vGluT1, but neither of the two GADs (**Figure 5C**). Markers of interneurons were rarely observed<sup>5,42,46</sup>. COX-2, chiefly expressed by layer II-III pyramidal cells<sup>3,16</sup>, was not detected in layer V pyramidal cells. The ATP1 $\alpha$ 1 and 3 subunits were more frequently observed than the ATP1 $\alpha$ 2 subunit<sup>3</sup>. The Kir6.2 and SUR1 subunits were rarely detected in layer V pyramidal neurons, which is consistent with their preferential expression in upper layers<sup>3,43</sup>. Care was taken not to harvest the nuclei, resulting in a rare detection of SOM introns (3 out of 26 cells, *i.e.*, 12%).

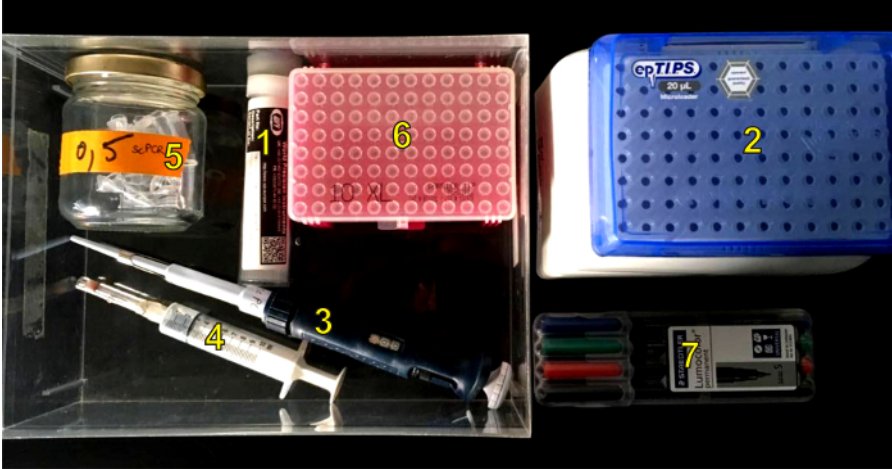


**Figure 1: Dedicated box for single cell RT-PCR.** List of materials reserved for RT-PCR after patch-clamp. (1) Borosilicate glass capillaries, (2) 20 µL long, fine, flexible tips, (3) 20 µL micropipette, (4) home-made expeller, (5) 500 µL PCR tubes, (6) 10 µL aerosol resistant filter tips, and (7) permanent markers. [Please click here to view a larger version of this figure.](#)

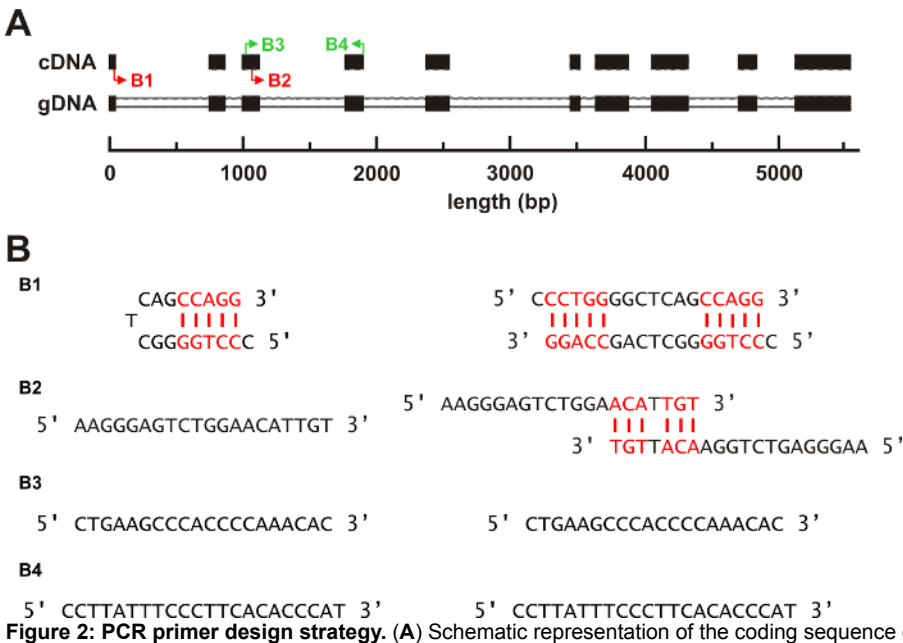


**Figure 2: PCR primer design strategy.** (A) Schematic representation of the coding sequence of COX 2 cDNA aligned to the mouse chromosome 2 sequence containing the COX 2 gene. Exons are represented by black boxes and introns on gDNA by white boxes. Note the gaps in the cDNA corresponding to the intronic sequences on gDNA. Representative examples of bad and good oligonucleotides represented as red and green arrows, respectively. Right and left arrows denote forward and reverse primers. (B) Sequences and secondary structures of the oligonucleotides shown in (A). Left and right panels indicate hairpin self-complementarity and self-dimer formation, respectively. The **B1** oligonucleotide displays both a strong hairpin self-complementarity and dimer formation whereas the **B2** oligonucleotide only shows dimer formation. Both **B3** and **B4** oligonucleotides have no hairpin self-complementarity and no dimer formation; they are intron overspanning (A) and have been selected as potential PCR primers (see **Table 1**). [Please click here to view a larger version of this figure.](#)

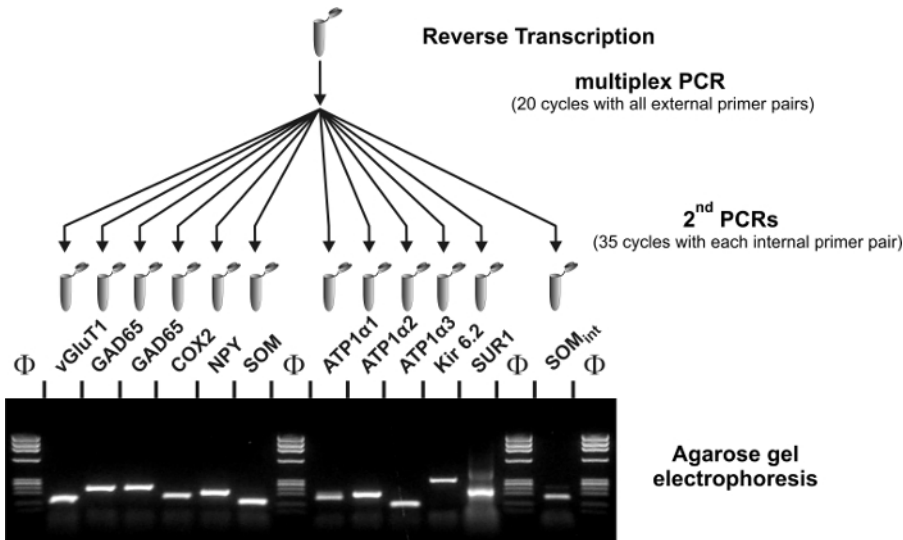


**Figure 3: Validation of multiplex PCR.** 1 ng of total RNA from mouse whole brain was subjected to a reverse transcription followed by two rounds of PCR amplification. The 12 PCR products were resolved in separate lanes by agarose gel electrophoresis in parallel with  $\Phi$ x174 digested by *Hae*III. The second PCR products had sizes (in bp) predicted by the sequences: 153 (vGluT1), 248 (GAD65), 255 (GAD67), 181 (COX 2), 220 (NPY), 146 (SOM), 183 (ATP1a1), 213 (ATP1a2), 128 (ATP1a3), 342 (Kir6.2), 211 (SUR1), and 182 (SOM<sub>int</sub>). [Please click here to view a larger version of this figure.](#)

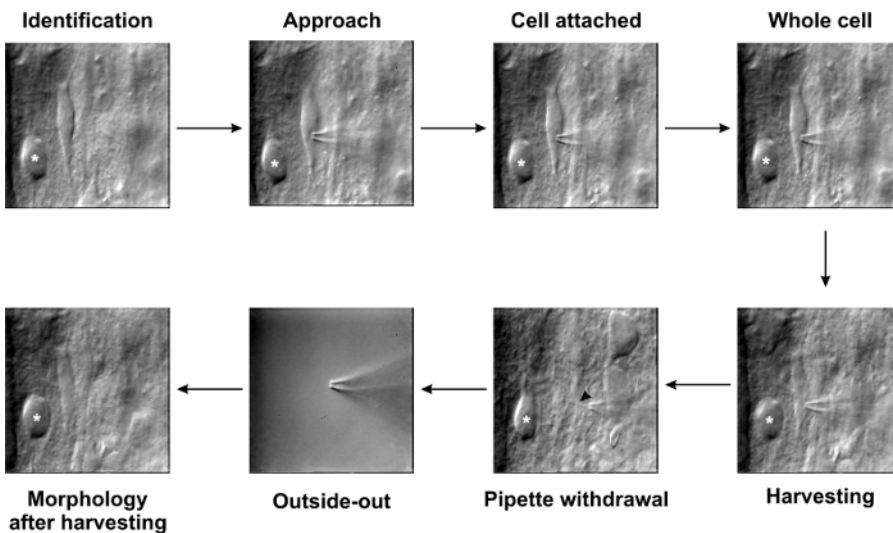


**Figure 4: Patch-clamp harvesting in brain slices.** Once a cell is visually identified, the recording pipette is approached with a positive pressure in order to avoid cellular debris contamination at the tip of the pipette. Note the dimple on the membrane of this neuron. Positive pressure is then interrupted in order to form a cell-attached configuration with a Gigaohm tight seal. Brief suction is applied to switch to whole-cell configuration. At the end of the recording, the cytoplasm is harvested by applying a gentle negative pressure into the pipette while maintaining the tight seal. Note the shrinkage of the cell body during the harvesting procedure. The recording pipette is then gently withdrawn to form an outside-out patch, which favors cell membrane closure for subsequent biocytin revelation, and preservation of harvested material in the patch pipette. Reproduced from Cauli and Lambolez<sup>47</sup> with permission from the Royal Society of Chemistry. [Please click here to view a larger version of this figure.](#)

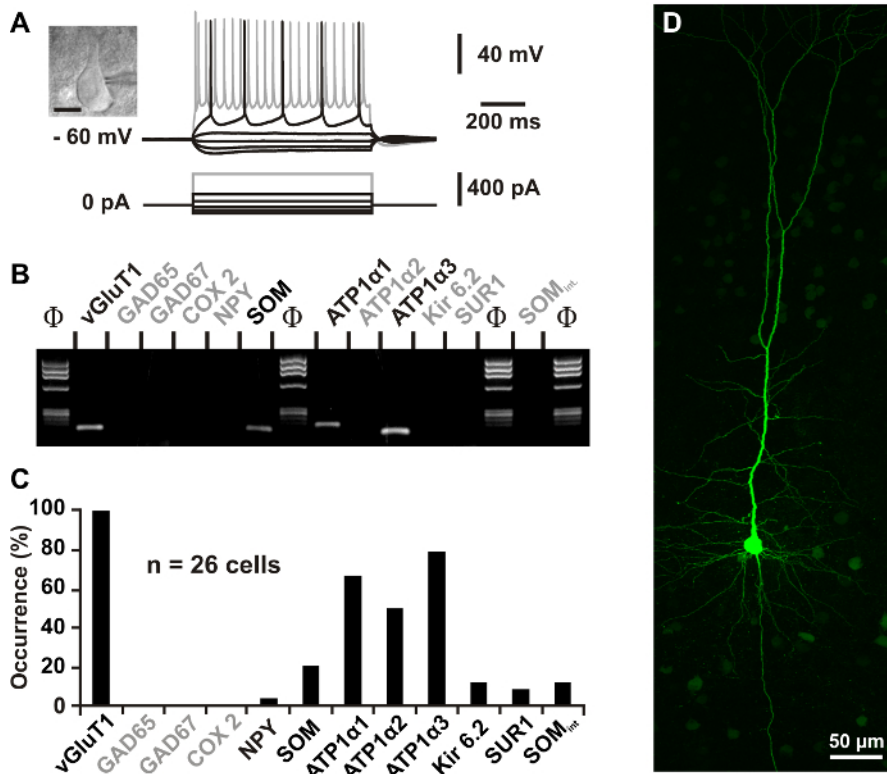


**Figure 5: Characterization of layer V neocortical pyramidal cells.** (A) Membrane potential response of the same cell induced by current pulses of -100, -40, -10, +60, +120, and +500 pA (bottom traces). The neuron displays a weak potential deflection after the initial hyperpolarizing response (upper traces). In response to a supraliminal depolarization, the neuron discharged long-lasting action potentials with slowly developing after-hyperpolarization (upper trace). Near saturation, the neuron discharged at a low frequency and exhibited a pronounced adaptation (upper gray trace). **Inset:** infrared pictures of the recorded layer V pyramidal neuron. The pial surface is upward. Scale bar: 20  $\mu$ m. (B) Multiplex RT-PCR analysis revealing expression of vGluT1, SOM, ATP1 $\alpha$ 1, and ATP1 $\alpha$ 3. (C) Gene expression profile in a sample of 26 layer V pyramidal cells. vGluT1 was expressed in all neurons while GAD65, GAD67, and COX2 were never detected. NPY, SOM, Kir6.2, SUR1, and SOM<sub>int</sub> were rarely observed. Pyramidal cells expressed ATP1 $\alpha$ 3, 1 subunit of the Na<sup>+</sup>/K<sup>+</sup> ATPase, and ATP1 $\alpha$ 2 to a lesser extent. (D) Maximum intensity projection of confocal images showing biocytin labeling of the neuron recorded in (A). [Please click here to view a larger version of this figure.](#)

| Gene / GenBank number             | External primers         | Size (bp)  | Internal primers       | Size (bp)  |
|-----------------------------------|--------------------------|------------|------------------------|------------|
| <b>vGlut1</b><br><b>NM_182993</b> | Sense, -113              | <b>259</b> | Sense, -54             | <b>153</b> |
|                                   | GGCTCCTTTTTCTGGGGCTAC    |            | ATTCGCAGCCAACAGGGTCT   |            |
|                                   | Anti-sense, 126          |            | Anti-sense, 79         |            |
|                                   | CCAGCCGACTCCGTCTAAG      |            | TGGCAAGCAGGGTATGTGAC   |            |
| <b>GAD65</b><br><b>NM_008078</b>  | Sense, 99                | <b>375</b> | Sense, 219             | <b>248</b> |
|                                   | CCAAAAGTTCACGGGCGG       |            | CACCTGCGACCAAAAACCCT   |            |
|                                   | Anti-sense, 454          |            | Anti-sense, 447        |            |
|                                   | TCCTCCAGATTTTGC GGTTG    |            | GATTTTGC GGTTGGTCTGCC  |            |
| <b>GAD67</b><br><b>NM_008077</b>  | Sense, 529               | <b>598</b> | Sense, 801             | <b>255</b> |
|                                   | TACGGGGTTCGCACAGGTC      |            | CCCAGAAGTGAAGACAAAAGGC |            |
|                                   | Anti-sense, 1109         |            | Anti-sense, 1034       |            |
|                                   | CCCAGGCAGCATCCACAT       |            | AATGCTCCGTAAACAGTCGTGC |            |
| <b>COX 2</b><br><b>NM_011198</b>  | Sense, 199               | <b>268</b> | Sense, 265             | <b>181</b> |
|                                   | CTGAAGCCCACCCAAACAC      |            | AACAACATCCCCTTCTCTGCG  |            |
|                                   | Anti-sense, 445          |            | Anti-sense, 426        |            |
|                                   | CCTTATTTCCCTTCACACCCAT   |            | TGGGAGTTGGGCAGTCATCT   |            |
| <b>NPY</b><br><b>NM_023456</b>    | Sense, 16                | <b>294</b> | Sense, 38              | <b>220</b> |
|                                   | CGAATGGGGCTGTGTGGA       |            | CCCTCGCTCTATCTCTGCTCGT |            |
|                                   | Anti-sense, 286          |            | Anti-sense, 236        |            |
|                                   | AAGTTTCATTTCCCATCACCACAT |            | GCGTTTTCTGTGCTTTCCTTCA |            |
| <b>SOM</b><br><b>NM_009215</b>    | Sense, 43                | <b>208</b> | Sense, 75              | <b>146</b> |
|                                   | ATCGTCCTGGCTTTGGGC       |            | GCCCTCGGACCCAGACT      |            |
|                                   | Anti-sense, 231          |            | Anti-sense, 203        |            |
|                                   | GCCTCATCTCGTCTGCTCA      |            | GCAAATCCTCGGGCTCCA     |            |
| <b>ATP1α1</b><br><b>NM_144900</b> | Sense, 1287              | <b>288</b> | Sense, 1329            | <b>183</b> |
|                                   | CAGGGCAGTGTTTCAGGCTAA    |            | TAAGCGGGCAGTAGCGGG     |            |
|                                   | Anti-sense, 1556         |            | Anti-sense, 1492       |            |
|                                   | CCGTGGAGAAGGATGGAGC      |            | AGGTGTTTGGGCTCAGATGC   |            |
| <b>ATP1α2</b><br><b>NM_178405</b> | Sense, 1392              | <b>268</b> | Sense, 1430            | <b>213</b> |
|                                   | AGTGAGGAAGATGAGGGACAGG   |            | AAATCCCCTTCAACTCCACCA  |            |
|                                   | Anti-sense, 1640         |            | Anti-sense, 1623       |            |
|                                   | ACAGAAGCCCAGCACTCGTT     |            | GTTCCCAAGTCTCCACAGC    |            |
| <b>ATP1α3</b><br><b>NM_144921</b> | Sense, 127               | <b>216</b> | Sense, 158             | <b>128</b> |
|                                   | CGGAAATACAATACTGACTGCGTG |            | TGACACACAGTAAAGCCCAGGA |            |
|                                   | Anti-sense, 324          |            | Anti-sense, 264        |            |
|                                   | GTCATCTCCGTCCCTGCC       |            | CCACAGCAGGATAGAGAAGCCA |            |
| <b>Kir6.2</b><br><b>NM_010602</b> | Sense, 306               | <b>431</b> | Sense, 339             | <b>342</b> |
|                                   | CGGAGAGGGCACCAATGT       |            | CATCCACTCCTTTTCATCTGCC |            |
|                                   | Anti-sense, 719          |            | Anti-sense, 663        |            |
|                                   | CACCCACGCCATTCTCCA       |            | TCGGGGCTGGTGGTCTTG     |            |
| <b>SUR1</b><br><b>NM_011510</b>   | Sense, 1867              | <b>385</b> | Sense, 2041            | <b>211</b> |
|                                   | CAGTGTGCCCCCGAGAG        |            | ATCATCGGAGGCTTCTTACC   |            |
|                                   | Anti-sense, 2231         |            | Anti-sense, 2231       |            |
|                                   | GGTCTTCTCCCTCGCTGTCTG    |            | GGTCTTCTCCCTCGCTGTCTG  |            |

|                          |                      |            |                      |            |
|--------------------------|----------------------|------------|----------------------|------------|
| <b>SOMint<br/>X51468</b> | Sense, 8             | <b>240</b> | Sense, 16            | <b>182</b> |
|                          | CTGTCCCCCTTACGAATCCC |            | CTTACGAATCCCCAGCCTT  |            |
|                          | Anti-sense, 228      |            | Anti-sense, 178      |            |
|                          | CCAGCACCAGGGATAGAGCC |            | TTGAAAGCCAGGGAGGAACT |            |

**Table 1. Sequences of first and second PCR primers.** The position of each PCR primer and their sequences are given from 5' to 3'. Except for the somatostatin intron, position 1 corresponds to the first base of the start codon of each gene.

## Discussion

Single cell multiplex RT-PCR after patch-clamp can simultaneously and reliably probe the expression of more than 30 genes in electrophysiologically identified cells<sup>5</sup>. Analyzing gene expression at the single cell level requires highly efficient PCR primers. One of the most limiting steps is collection of the cell's content. Its efficiency depends on the diameter of the patch pipette tip, which must be as large as possible while matching the cell size. Pipettes with a 1-2  $\mu\text{m}$  open tip diameter were proven to be suitable for most neuronal types. It is also essential to make sure that only the cellular content is collected, and not the surrounding tissue. This is achieved by controlling electrophysiologically the preservation of a tight seal during the harvest. The formation of an outside-out patch configuration during pipette withdrawal further protects the harvested cytoplasm from cellular debris. The success rate of the single cell multiplex RT-PCR also depends on mRNAs abundance of the investigated cell type. For instance, the yield obtained with astrocytes, which express mRNAs in relatively low amounts<sup>3</sup>, is generally lower than the one obtained with neurons and thus requires increasing sample size<sup>15,16</sup>. Reverse transcription, which has a low efficiency in tubes<sup>48</sup>, is the limiting reaction of single cell multiplex RT-PCR. It is therefore critical to use top quality reagents, to store them as aliquots at  $-80\text{ }^{\circ}\text{C}$ , and to use them only for one day. Finally, the DNA polymerase activity of the RTase is often an overlooked source of primer-dimer formation. To address this issue, performing a hot start with primers is critical to increase the amplification efficiency. In addition this will reduce the inhibitory effect of RTase on the Taq DNA polymerase activity<sup>49</sup>.

The single cell multiplex RT-PCR technique is highly versatile. It has been extensively used in rodents<sup>10,11,13,19,20,34,50,51,52,53,54</sup> but can be adapted to virtually all animal models and genes assuming that tissue and gene sequences are available. Various patch-clamp solutions can be used as long as they do not interfere with the RT-PCR on cell free assays. For instance internal solutions based on  $\text{K}^+$  or  $\text{Cs}^+$  cations,  $\text{Cl}^-$  or gluconate have been successfully used<sup>6,36,41,55</sup>.

Classical false negative results stem from RNase contamination of the patch pipette filament and/or internal patch-clamp solution. Carefully chlorinating the filament and validating the internal solution generally solve this problem. False negative results can also occur when a gene is expressed at a low single cell level, since only a proportion of the cytoplasm is harvested. The harvesting quality can be increased by using larger pipettes and/or by reducing the time of the whole-cell recording. Harvesting quality can be assessed by including a gene known to be expressed at a particular level in single cells<sup>20</sup>. False positive results can occur with bad tissue quality, in which the amount of contaminating cellular debris is high. Testing the presence of debris is done by inserting a patch pipette into the slice without performing any seal and releasing the positive pressure prior to the pipette removal. The presence of amplifiable materials is then probed by multiplex RT-PCR<sup>42</sup>. Silanizing the patch pipette has also been used to reduce the collection of extracellular contaminants<sup>56</sup>. Single cell PCR is a very sensitive technique that can detect as little as a single copy of double stranded DNA<sup>57</sup>. In the case of intron-less genes, the gDNA contained in the nucleus can also produce false positives. Avoiding the collection of gDNA by placing the pipette away from the nucleus during the harvesting helps to solve this issue. The presence of gDNA can be reliably probed by amplifying an intronic sequence<sup>25</sup>.

The detection of mRNA molecules by RT-PCR becomes unreliable at 10 copies<sup>44</sup>, presumably because of the low efficiency of the RTase<sup>48</sup>, and can lead to an under detection of low-abundance transcripts<sup>26,42</sup>. This can be problematic in the case of intron-less genes. Indeed, avoiding harvest of the nucleus reduces the amount of cytoplasm that can be collected and therefore the detection sensitivity. The combination of single-cell RT-PCR after patch-clamp with biocytin labeling requires that the shape of the cell is maintained as much as possible (**Figure 3**). Unavoidably, this reduces the amount of material that can be collected, thereby reducing the success rate. A compromise between cytoplasm collection and preservation of cell morphology is mandatory.

Multiplex single-cell RT-PCR data are not quantitative as they only give information on whether cDNAs are present or absent in the collected material. However, because of the detection limits described above, the occurrence of detection at the population level can reflect the abundance of genes at the single cell level. Alternative approaches allow the generation of more quantitative data, but the technical constraints imposed by their specific amplification strategies (*i.e.*, relative quantification of homologous genes or RT-qPCR) largely restrict the number of genes that can be simultaneously analyzed<sup>41,53,55,58,59,60,61,62,63,64,65,66</sup>. The recent combination of patch-clamp recordings and single cell RNaseq, referred to as Patch-seq<sup>30,31</sup>, allows quantitative transcriptomic analysis of electrophysiologically-characterized cells. It is a new and promising approach, yet it requires access to high-throughput sequencers and the data generated require time consuming analysis.

## Disclosures

The authors have nothing to disclose.

## Acknowledgements

We thank Dr. Alexandre Mouro for his comments on the manuscript. This work was supported by grants from the Agence Nationale de la Recherche (ANR 2011 MALZ 003 01; ANR-15-CE16-0010 and ANR-17-CE37-0010-03), BLG is supported by fellowship from the Fondation pour la Recherche sur Alzheimer. We thank the animal facility of the IBPS (Paris, France).

## References

1. Ascoli, G.A. *et al.* Petilla terminology: nomenclature of features of GABAergic interneurons of the cerebral cortex. *Nat.Rev.Neurosci.* **9** (7), 557-568, (2008).
2. DeFelipe, J. *et al.* New insights into the classification and nomenclature of cortical GABAergic interneurons. *Nat.Rev.Neurosci.* (2013).
3. Tasic, B. *et al.* Adult mouse cortical cell taxonomy revealed by single cell transcriptomics. *Nat.Neurosci.* (2016).
4. Zeisel, A. *et al.* Cell types in the mouse cortex and hippocampus revealed by single-cell RNA-seq. *Science.* (2015).
5. Cauli, B. *et al.* Classification of fusiform neocortical interneurons based on unsupervised clustering. *Proc.Natl.Acad.Sci.U.S.A.* **97** (11), 6144-6149, (2000).
6. Cauli, B. *et al.* Molecular and physiological diversity of cortical nonpyramidal cells. *J.Neurosci.* **17** (10), 3894-3906, (1997).
7. Férézou, I. *et al.* 5-HT<sub>3</sub> receptors mediate serotonergic fast synaptic excitation of neocortical vasoactive intestinal peptide/cholecystokinin interneurons. *J. Neurosci.* **22** (17), 7389-7397, (2002).
8. Cauli, B. *et al.* Cortical GABA interneurons in neurovascular coupling: relays for subcortical vasoactive pathways. *J.Neurosci.* **24** (41), 8940-8949, (2004).
9. Wang, Y., Gupta, A., Toledo-Rodriguez, M., Wu, C.Z., & Markram, H. Anatomical, physiological, molecular and circuit properties of nest basket cells in the developing somatosensory cortex. *Cereb.Cortex.* **12** (4), 395-410, (2002).
10. Wang, Y. *et al.* Anatomical, physiological and molecular properties of Martinotti cells in the somatosensory cortex of the juvenile rat. *J.Physiol.* **561** (Pt 1), 65-90, (2004).
11. Karagiannis, A. *et al.* Classification of NPY-expressing neocortical interneurons. *J.Neurosci.* **29** (11), 3642-3659, (2009).
12. Battaglia, D., Karagiannis, A., Gallopin, T., Gutch, H.W., & Cauli, B. Beyond the frontiers of neuronal types. *Front Neural Circuits.* **7** 13, (2013).
13. Toledo-Rodriguez, M. *et al.* Correlation maps allow neuronal electrical properties to be predicted from single-cell gene expression profiles in rat neocortex. *Cereb.Cortex.* **14** (12), 1310-1327, (2004).
14. Toledo-Rodriguez, M., Goodman, P., Illic, M., Wu, C., & Markram, H. Neuropeptide and calcium binding protein gene expression profiles predict neuronal anatomical type in the juvenile rat. *J.Physiol.* (2005).
15. Lecrux, C. *et al.* Pyramidal neurons are "neurogenic hubs" in the neurovascular coupling response to whisker stimulation. *J.Neurosci.* **31** (27), 9836-9847, (2011).
16. Lacroix, A. *et al.* COX-2-derived prostaglandin E<sub>2</sub> produced by pyramidal neurons contributes to neurovascular coupling in the rodent cerebral cortex. *J.Neurosci.* **35** (34), 11791-11810, (2015).
17. Mathias, K. *et al.* Segregated expression of AMPA-type glutamate receptors and glutamate transporters defines distinct astrocyte populations in the mouse hippocampus. *J.Neurosci.* **23** (5), 1750-1758, (2003).
18. Rancillac, A. *et al.* Glutamatergic control of microvascular tone by distinct gaba neurons in the cerebellum. *J.Neurosci.* **26** (26), 6997-7006, (2006).
19. Miki, T. *et al.* ATP-sensitive K<sup>+</sup> channels in the hypothalamus are essential for the maintenance of glucose homeostasis. *Nat.Neurosci.* **4** (5), 507-512, (2001).
20. Liss, B., Bruns, R., & Roeper, J. Alternative sulfonylurea receptor expression defines metabolic sensitivity of K-ATP channels in dopaminergic midbrain neurons. *EMBO J.* **18** (4), 833-846, (1999).
21. Gallopin, T. *et al.* Identification of sleep-promoting neurons in vitro. *Nature.* **404** (6781), 992-995, (2000).
22. Gallopin, T. *et al.* The endogenous somnogen adenosine excites a subset of sleep-promoting neurons via A<sub>2A</sub> receptors in the ventrolateral preoptic nucleus. *Neuroscience.* **134** (4), 1377-1390, (2005).
23. Fernandez, S.P. *et al.* Multiscale single-cell analysis reveals unique phenotypes of raphe 5-HT neurons projecting to the forebrain. *Brain Struct.Funct.* (2015).
24. Porter, J.T. *et al.* Selective excitation of subtypes of neocortical interneurons by nicotinic receptors. *J.Neurosci.* **19** (13), 5228-5235, (1999).
25. Hill, E.L. *et al.* Functional CB<sub>1</sub> receptors are broadly expressed in neocortical GABAergic and glutamatergic neurons. *J.Neurophysiol.* **97** (4), 2580-2589, (2007).
26. Férézou, I. *et al.* Extensive overlap of mu-opioid and nicotinic sensitivity in cortical interneurons. *Cereb.Cortex.* **17** (8), 1948-1957, (2007).
27. Hu, E. *et al.* VIP, CRF, and PACAP act at distinct receptors to elicit different cAMP/PKA dynamics in the neocortex. *Cereb.Cortex.* **21** (3), 708-718, (2011).
28. Louessard, M. *et al.* Tissue plasminogen activator expression is restricted to subsets of excitatory pyramidal glutamatergic neurons. *Mol.Neurobiol.* (2015).
29. Stuart, G.J., Dodt, H.U., & Sakmann, B. Patch-clamp recordings from the soma and dendrites of neurons in brain slices using infrared video microscopy. *Pflugers Arch.* **423** (5-6), 511-8, (1993).
30. Cadwell, C.R. *et al.* Electrophysiological, transcriptomic and morphologic profiling of single neurons using Patch-seq. *Nat.Biotechnol.* **34** (2), 199-203, (2016).
31. Fuzik, J. *et al.* Integration of electrophysiological recordings with single-cell RNA-seq data identifies neuronal subtypes. *Nat.Biotechnol.* **34** (2), 175-183, (2016).
32. O'Leary, N.A. *et al.* Reference sequence (RefSeq) database at NCBI: current status, taxonomic expansion, and functional annotation. *Nucleic Acids Res.* **44** (D1), D733-D745, (2016).
33. Schuler, G.D., Altschul, S.F., & Lipman, D.J. A workbench for multiple alignment construction and analysis. *Proteins.* **9** (3), 180-190, (1991).
34. Ruano, D., Lambolez, B., Rossier, J., Paternain, A.V., & Lerma, J. Kainate receptor subunits expressed in single cultured hippocampal neurons: molecular and functional variants by RNA editing. *Neuron.* **14** (5), 1009-1017, (1995).
35. Porter, J.T. *et al.* Properties of bipolar VIPergic interneurons and their excitation by pyramidal neurons in the rat neocortex. *Eur.J.Neurosci.* **10** (12), 3617-3628, (1998).
36. Ruano, D., Perrais, D., Rossier, J., & Ropert, N. Expression of GABA(A) receptor subunit mRNAs by layer V pyramidal cells of the rat primary visual cortex. *Eur.J.Neurosci.* **9** (4), 857-862, (1997).
37. Altschul, S.F., Gish, W., Miller, W., Myers, E.W., & Lipman, D.J. Basic local alignment search tool. *J.Mol.Biol.* **215** (3), 403-410, (1990).

38. Chomczynski, P., & Sacchi, N. Single-step method of RNA isolation by acid guanidinium thiocyanate- phenol-chloroform extraction. *Anal Biochem.* **162** (1), 156-9, (1987).
39. Lee, P.Y., Costumbrado, J., Hsu, C.Y., & Kim, Y.H. Agarose gel electrophoresis for the separation of DNA fragments. *J. Vis. Exp.* (62), (2012).
40. Liss, B. *et al.* K-ATP channels promote the differential degeneration of dopaminergic midbrain neurons. *Nat. Neurosci.* **8** (12), 1742-1751, (2005).
41. Lambolez, B., Audinat, E., Bochet, P., Crepel, F., & Rossier, J. AMPA receptor subunits expressed by single Purkinje cells. *Neuron.* **9** (2), 247-258, (1992).
42. Gallopin, T., Geoffroy, H., Rossier, J., & Lambolez, B. Cortical sources of CRF, NKB, and CCK and their effects on pyramidal cells in the neocortex. *Cereb. Cortex.* **16** (10), 1440-1452, (2006).
43. Cunningham, M.O. *et al.* Neuronal metabolism governs cortical network response state. *Proc. Natl. Acad. Sci. U.S.A.* **103** (14), 5597-5601, (2006).
44. Tsuzuki, K., Lambolez, B., Rossier, J., & Ozawa, S. Absolute quantification of AMPA receptor subunit mRNAs in single hippocampal neurons. *J. Neurochem.* **77** (6), 1650-1659, (2001).
45. McCormick, D.A., Connors, B.W., Lighthall, J.W., & Prince, D.A. Comparative electrophysiology of pyramidal and sparsely spiny stellate neurons of the neocortex. *Journal of Neurophysiology.* **54** (4), 782-806, (1985).
46. Andjelic, S. *et al.* Glutamatergic nonpyramidal neurons from neocortical layer VI and their comparison with pyramidal and spiny stellate neurons. *J. Neurophysiol.* **101** (2), 641-654, (2009).
47. Cauli, B., & Lambolez, B. In: *Unravelling Single Cell Genomics: Micro and Nanotools*. RSC Nanoscience and Nanotechnology. Bontoux, N., & Potier, M.C. eds., Ch. 9, RSC publishing, Cambridge, 81-92 (2010).
48. Bontoux, N. *et al.* Integrating whole transcriptome assays on a lab-on-a-chip for single cell gene profiling. *Lab Chip.* **8** (3), 443-450 (2008).
49. Sellner, L.N., Coelen, R.J., & Mackenzie, J.S. Reverse transcriptase inhibits Taq polymerase activity. *Nucleic Acids Res.* **20** (7), 1487-1490, (1992).
50. Perrenoud, Q., Rossier, J., Geoffroy, H., Vitalis, T., & Gallopin, T. Diversity of GABAergic interneurons in layer VIa and VIb of mouse barrel cortex. *Cereb. Cortex.* (2012).
51. Tricoire, L. *et al.* Common origins of hippocampal ivy and nitric oxide synthase expressing neurogliaform cells. *J. Neurosci.* **30** (6), 2165-2176, (2010).
52. Cea-del Rio, C.A. *et al.* M3 muscarinic acetylcholine receptor expression confers differential cholinergic modulation to neurochemically distinct hippocampal basket cell subtypes. *J. Neurosci.* **30** (17), 6011-6024 [doi] (2010).
53. Tricoire, L. *et al.* A blueprint for the spatiotemporal origins of mouse hippocampal interneuron diversity. *J. Neurosci.* **31** (30), 10948-10970 [doi] (2011).
54. Franz, O., Liss, B., Neu, A., & Roeper, J. Single-cell mRNA expression of HCN1 correlates with a fast gating phenotype of hyperpolarization-activated cyclic nucleotide-gated ion channels (Ih) in central neurons. *Eur. J. Neurosci.* **12** (8), 2685-2693, (2000).
55. Szabo, A. *et al.* Calcium-permeable AMPA receptors provide a common mechanism for LTP in glutamatergic synapses of distinct hippocampal interneuron types. *J. Neurosci.* **32** (19), 6511-6516 [doi] (2012).
56. Hodne, K., & Weltzien, F.A. Single-Cell Isolation and Gene Analysis: Pitfalls and Possibilities. *Int. J. Mol. Sci.* **16** (11), 26832-26849, (2015).
57. Li, H.H. *et al.* Amplification and analysis of DNA sequences in single human sperm and diploid cells. *Nature.* **335** (6189), 414-417, (1988).
58. Bochet, P. *et al.* Subunit composition at the single-cell level explains functional properties of a glutamate-gated channel. *Neuron.* **12** (2), 383-388, (1994).
59. Audinat, E., Lambolez, B., Rossier, J., & Crepel, F. Activity-dependent regulation of N-methyl-D-aspartate receptor subunit expression in rat cerebellar granule cells. *Eur. J. Neurosci.* **6** (12), 1792-1800, (1994).
60. Jonas, P., Racca, C., Sakmann, B., Seeburg, P.H., & Monyer, H. Differences in Ca<sup>2+</sup> permeability of AMPA-type glutamate receptor channels in neocortical neurons caused by differential GluR-B subunit expression. *Neuron.* **12** (6), 1281-1289, (1994).
61. Geiger, J.R. *et al.* Relative abundance of subunit mRNAs determines gating and Ca<sup>2+</sup> permeability of AMPA receptors in principal neurons and interneurons in rat CNS. *Neuron.* **15** (1), 193-204, (1995).
62. Flint, A.C., Maisch, U.S., Weishaupt, J.H., Kriegstein, A.R., & Monyer, H. NR2A subunit expression shortens NMDA receptor synaptic currents in developing neocortex. *J. Neurosci.* **17** (7), 2469-2476, (1997).
63. Angulo, M.C., Lambolez, B., Audinat, E., Hestrin, S., & Rossier, J. Subunit composition, kinetic, and permeation properties of AMPA receptors in single neocortical nonpyramidal cells. *J. Neurosci.* **17** (17), 6685-6696, (1997).
64. Lambolez, B., Ropert, N., Perrais, D., Rossier, J., & Hestrin, S. Correlation between kinetics and RNA splicing of alpha-amino-3-hydroxy-5-methylisoxazole-4-propionic acid receptors in neocortical neurons. *Proc. Natl. Acad. Sci. U.S.A.* **93** (5), 1797-1802, (1996).
65. Liss, B. *et al.* Tuning pacemaker frequency of individual dopaminergic neurons by Kv4.3L and KChip3.1 transcription. *EMBO J.* **20** (20), 5715-5724, (2001).
66. Aponte, Y., Lien, C.C., Reisinger, E., & Jonas, P. Hyperpolarization-activated cation channels in fast-spiking interneurons of rat hippocampus. *J. Physiol.* **574** (Pt 1), 229-243, (2006).